

# Near-infrared low-resolution spectroscopy of Pleiades L-type brown dwarfs

G. Bihain<sup>1,2</sup>, R. Rebolo<sup>1,2,3</sup>, M. R. Zapatero Osorio<sup>4</sup>, V. J. S. Béjar<sup>1,3</sup>, and J. A. Caballero<sup>5,4</sup>

<sup>1</sup> Instituto de Astrofísica de Canarias, c/ Vía Láctea, s/n, 38205 La Laguna, Tenerife, Islas Canarias, Spain  
e-mail: gbihain@iac.es

<sup>2</sup> Consejo Superior de Investigaciones Científicas (CSIC), Spain

<sup>3</sup> Departamento de Astrofísica, Universidad de La Laguna, 38205 La Laguna, Tenerife, Islas Canarias, Spain

<sup>4</sup> Centro de Astrobiología (CSIC-INTA), Carretera de Ajalvir, km 4. E-28850 Torrejón de Ardoz, Madrid, Spain.

<sup>5</sup> Dpto. de Astrofísica y Ciencias de la Atmósfera, Facultad de Física, Universidad Complutense de Madrid, E-28040 Madrid, Spain

Received 15 November 2009 / accepted 18 May 2010

## ABSTRACT

**Context.** The fundamental properties of brown dwarfs evolve with age. Models describing the evolution of luminosities and effective temperatures, among other physical parameters, can be empirically constrained using brown dwarfs of various masses in star clusters of well determined age and metallicity.

**Aims.** We aim to carry out a spectroscopic and photometric characterization of low-mass brown dwarfs of the ~120 Myr old Pleiades open cluster.

**Methods.** We obtained low-resolution near-infrared spectra of the  $J = 17.4$ – $18.8$  mag candidate L-type brown dwarfs PLIZ 28 and 35, BRB 17, 21, 23, and 29, which are Pleiades members by photometry and proper motion. We also obtained spectra of the well-known  $J = 15.4$ – $16.1$  mag late M-type cluster members PPI 1, Teide 1, and Calar 3.

**Results.** We find that the former six objects have early- to mid-L spectral types and confirm previously reported M-types for the other three objects. The spectra of the L0-type BRB 17 and PLIZ 28 present a triangular  $H$ -band continuum shape, indicating that this peculiar spectral feature persists until at least the age of the Pleiades. We add to our sample 36 reported M5–L0-type cluster members, collecting their  $I_C$ - and UKIDSS  $ZYJHK$ -band photometry. We confirm a possible interleaving of the Pleiades and field L-type sequences in the  $JHK$  absolute magnitude versus spectral type diagrams, and quantify marginally redder Pleiades  $J - K$  colours, by  $0.11 \pm 0.20$  mag, possibly related to both reddening and youth. Using field dwarf bolometric correction – and effective temperature – spectral type relations, we obtain the Hertzsprung–Russell diagram of the Pleiades sample. Theoretical models reproduce well the spectral sequence at M5.5–9, but appear to overestimate the luminosity or underestimate the effective temperature at L0–5.

**Conclusions.** We classify six faint Pleiades brown dwarfs as early to mid L-type objects using low-resolution near-infrared spectra. We compare their properties to field dwarfs and theoretical models and estimate their masses to be in the range  $0.025$ – $0.035 M_{\odot}$ .

**Key words.** open clusters and associations: individual: Pleiades – stars: low-mass, brown dwarfs – stars: fundamental parameters (classification, colours, luminosities, masses, radii, temperatures)

## 1. Introduction

About 600 field L-type dwarfs have been spectroscopically identified to date.<sup>1</sup> Most of them have been discovered by large sky-area surveys such as 2MASS (Skrutskie et al. 2006) and SDSS (Abazajian et al. 2009). Spectroscopy has allowed the determination of physical properties and the derivation of effective temperatures (in the range ~2300–1400 K; e.g. Leggett et al. 2001), and parallax studies have provided distances and luminosities for about 10% of these objects, indicating that they are most probably very low mass stars or massive brown dwarfs. For individual field L-dwarfs, an estimation of mass from the luminosity and effective temperature requires additional information on age, which is in general difficult to obtain. This limits our ability to determine the field substellar mass function and formation history (Reid et al. 1999; Chabrier 2002, 2003; Kroupa & Bouvier 2003; Burgasser 2004; Allen et al. 2005; Pinfield et al. 2006).

An empirical determination of the evolution of effective temperature and luminosity with age for L-type dwarfs could be

obtained by identifying such objects in stellar associations of various ages. Brown dwarf- and planetary-mass candidates of (mostly early) L-type have been studied photometrically and spectroscopically in the Serpens (Lodieu et al. 2002), Ophiuchus (Jayawardhana & Ivanov 2006a), Chamaeleon I (Luhman et al. 2006, 2008; Luhman & Muench 2008; Schmidt et al. 2008), Chamaeleon II (Jayawardhana & Ivanov 2006b; Allers et al. 2007), Taurus (Itoh et al. 2005; Luhman et al. 2009), Trapezium (Lucas et al. 2001, 2006; Weights et al. 2009), and Lupus 1 clouds (Neuhäuser et al. 2005; McElwain et al. 2007), the  $\sigma$  Orionis open cluster (Zapatero Osorio et al. 1999a, 2000; Béjar et al. 2001; Martín et al. 2001; Barrado y Navascués et al. 2001, 2002; McGovern et al. 2004), and the TW Hydrae (Gizis 2002; Chauvin et al. 2004; Looper et al. 2007), Upper Scorpius (Lodieu et al. 2008; Lafrenière et al. 2008; Béjar et al. 2008), and Tucana–Horologium associations (Chauvin et al. 2005). All these star-forming regions are very young, with ages of a few Myr to a few tens of Myr. Finally, several L-type dwarfs characterized photometrically and spectroscopically have been associated with moving groups, such as the all-sky,  $400 \pm 100$  Myr

<sup>1</sup> <http://spider.ipac.caltech.edu/staff/davy/ARCHIVE/index.shtml>, 2010 May 17.

**Table 1.** Spectroscopic observations.

Object	$J^b$ (mag)	Opt. SpT <sup>c</sup>	Instrument <sup>d</sup>	Date	$T_{\text{exp}}^e$ (min)	Airmass	$\Delta\text{airmass}_{\text{T-S}}$	S/N <sup>f</sup>	Near-IR SpT
PPI 1	15.36±0.01	M6.5	NICS( <i>JHK</i> )	2002 Oct 31	8×2	1.08	0.14	50	M7.0±0.5
Calar 3	16.08±0.01	M8	NICS( <i>JHK</i> )	2002 Oct 31	8×2	1.15	0.07	49	M8.0±0.5
Teide 1	16.21±0.01	M8	NICS( <i>JHK</i> )	2002 Nov 27	8×2	1.03	0.73	32	M8.0±0.5
BRB 17	17.41±0.03	...	LIRIS( <i>zJ, HK</i> )	2006 Dec 28	(12, 18)×2	1.74, 1.41	0.44, 0.89	4, 6	L0.0±1.0
PLIZ 28	17.60±0.04	...	NICS( <i>JHK</i> )	2005 Nov 20	15×2	1.11	0.57	18	L0.0±1.0
PLIZ 35	18.07±0.05	...	NICS( <i>JHK</i> )	2005 Sep 18	65×0.6	1.03	-0.03	15	L2.0±1.0
BRB 21	18.14±0.06	...	NICS( <i>JHK</i> )	2005 Sep 18	80×0.5	1.21	0.15	7	L3.0±1.0
BRB 23	18.23±0.04	...	NICS( <i>JHK</i> )	2007 Feb 7	10×5	1.33	-0.27	14	L3.5±1.0
BRB 29	18.69±0.10	...	LIRIS( <i>HK</i> )	2006 Dec 29	12×2	1.09	-0.02	3	L4.5±1.5
J0829 <sup>a</sup>	12.80±0.03	L2V	LIRIS( <i>zJ, HK</i> )	2006 Dec 28	(4, 6)×1.5	1.38, 1.36	0.80, 0.94	29, 37	L2.0±1.0

(<sup>a</sup>) SSSPM J0829–1309. (<sup>b</sup>) From the Galactic Clusters Survey (GCS) component of UKIDSS (Lawrence et al. 2007, sixth data release) for the Pleiades members and from 2MASS (Skrutskie et al. 2006) for the field object. (<sup>c</sup>) From Martín et al. (1996) for the three Pleiades objects and from Scholz & Meusinger (2002) and Lodieu et al. (2005) for the field object. (<sup>d</sup>) A slit width of 1.0 arcsec was used, except for Calar 3 and PPI 1 (1.5 arcsec). The NICS/Amici spectra have a constant resolving power  $R = \lambda/\Delta\lambda \approx 50$  in the range 0.8–2.5  $\mu\text{m}$  (dispersion 3–10 nm pix<sup>-1</sup>); for Calar 3 and PPI 1,  $R \approx 33$ . The LIRIS *zJ*-band (0.887–1.531  $\mu\text{m}$ ) spectra have  $R \approx 960$  at  $\lambda \approx 1.17 \mu\text{m}$  and a dispersion of 0.61 nm pix<sup>-1</sup>, whereas the *HK*-band (1.388–2.419  $\mu\text{m}$ ) spectra have  $R \approx 945$  at  $\lambda \approx 1.83 \mu\text{m}$  and a dispersion of 0.97 nm pix<sup>-1</sup>. (<sup>e</sup>) Dithers × detector integration time. (<sup>f</sup>) Pseudo-continuum signal-to-noise ratios are measured in the interval 2.14–2.24  $\mu\text{m}$ , or for the LIRIS *zJ*-band data, in the interval 1.28–1.32  $\mu\text{m}$ .

old Ursa Major moving group (Bannister & Jameson 2007; Jameson et al. 2008; Casewell et al. 2008).

In this context, the Pleiades open cluster is well suited to provide a reference sequence for L- and T-dwarfs at an age of  $\sim 120$  Myr. Proper motion studies (Moraux et al. 2003; Bihain et al. 2006; Lodieu et al. 2007) have shown that there is a significant population of low-luminosity members of the cluster that, based on their optical and near-infrared colours, are likely to be of spectral type L. Casewell et al. (2007) have extended the brown dwarf search beyond these objects with some candidate members of spectral type T. Here, we report near-infrared spectroscopy for six of the nine L-type candidates confirmed as Pleiades proper motion members by Bihain et al. (2006), which allows us to study the relationship between spectral type and luminosity for L dwarfs at a homogeneous age and solar metallicity.

## 2. Observations and data reduction

Low-resolution spectra of four candidate L-type Pleiades brown dwarfs and three well-known late M-type Pleiads were obtained with the Near Infrared Camera Spectrometer (NICS) and its Amici prism, mounted on the 3.6 m Telescopio Nazionale Galileo (TNG; Observatorio del Roque de Los Muchachos – ORM–, Spain). Additional spectra of two other candidate L-type Pleiades brown dwarfs and an L2-type field dwarf were obtained with the Long-Slit Intermediate Resolution Infrared Spectrograph (LIRIS), mounted at the 4.2 m William Herschel Telescope (WHT; ORM). Table 1 lists the object names,  $J$ -band magnitudes, optical spectral types (when available), instruments (and bandpass coverage), observing-night dates, exposure times, mean airmasses, differences in mean airmasses between telluric standard stars (T) and the science objects (S), and pseudo-continuum signal-to-noise ratios. The weather conditions were clear, except on the nights of 2002 November 27 and 2006 December 28, when some clouds were present. The seeing was in the range 0.6–1.5 arcsec. Small dithers over two or three different positions along the slits were performed to allow for sky subtraction. Spectra of hot, B9–A1V stars were obtained during each observing night, except in 2002, when the spectra

of a DAO white dwarf and a K1 dwarf were obtained, relatively close in coordinates to the scientific targets, for the correction of the instrumental response and the telluric absorption.

The raw spectroscopic data were reduced using standard routines within the IRAF<sup>2</sup> environment. Amici spectra were sky-subtracted, flat-fielded, aligned, combined, optimally extracted, and wavelength calibrated using the look-up table provided in the instrument’s webpage<sup>3</sup> and the deep telluric absorption features. LIRIS raw images were corrected for pixel mapping and row cross-talk, and the spectra were sky-subtracted, flat-fielded, wavelength calibrated (using vacuum wavelengths of Ar arc lamps), shifted, and combined using routines in the LIRISDR package developed by J. A. Acosta-Pulido before they were optimally extracted. The instrumental response and telluric bands were removed dividing by the “telluric” spectra and multiplying by black-body spectra with the same effective temperature. The intrinsic lines in the LIRIS hot-star spectra were removed before dividing the science spectra. A vacuum-to-air correction was applied to the LIRIS spectra, using the default standard temperature and pressure. As indicated in the column  $\Delta\text{airmass}_{\text{T-S}}$  of Table 1, some of our science spectra were acquired at airmasses quite different to the telluric spectra, thus yielding a poor correction of telluric bands. The reduced Amici spectrum of BRB 23 was cut longwards of 2.245  $\mu\text{m}$  because the level of the sky counts entered the non-linear regime of the detector. The LIRIS *zJ* and *HK* spectra were flux calibrated using published *JH*-band photometry, allowing us to combine both parts.

## 3. Spectral types

In Figs 1 and 2, we show the reduced Amici and LIRIS spectra, respectively, and also a model atmospheric transmission (Hammersley 1998). The main absorption features of our target spectra are indicated (see Cushing et al. 2005 for details).

<sup>2</sup> IRAF is distributed by the National Optical Astronomy Observatories, which are operated by the Association of Universities for Research in Astronomy, Inc., under cooperative agreement with the National Science Foundation.

<sup>3</sup> <http://web.archive.org/web/20071126094610/http://www.tng.iac.es/instruments/nics/spectroscopy.html>

As expected for late M- and L-type objects, the spectra display intense water absorption bands at 1.3–1.51 and 1.75–2.05  $\mu\text{m}$ . Also, as expected for lower effective temperatures and dustier atmospheres (see Fig. 2 in Tsuji et al. 1996), the fainter objects have a flux at 0.85–1.3  $\mu\text{m}$  that is decreased compared to that at *H* or *K* band.

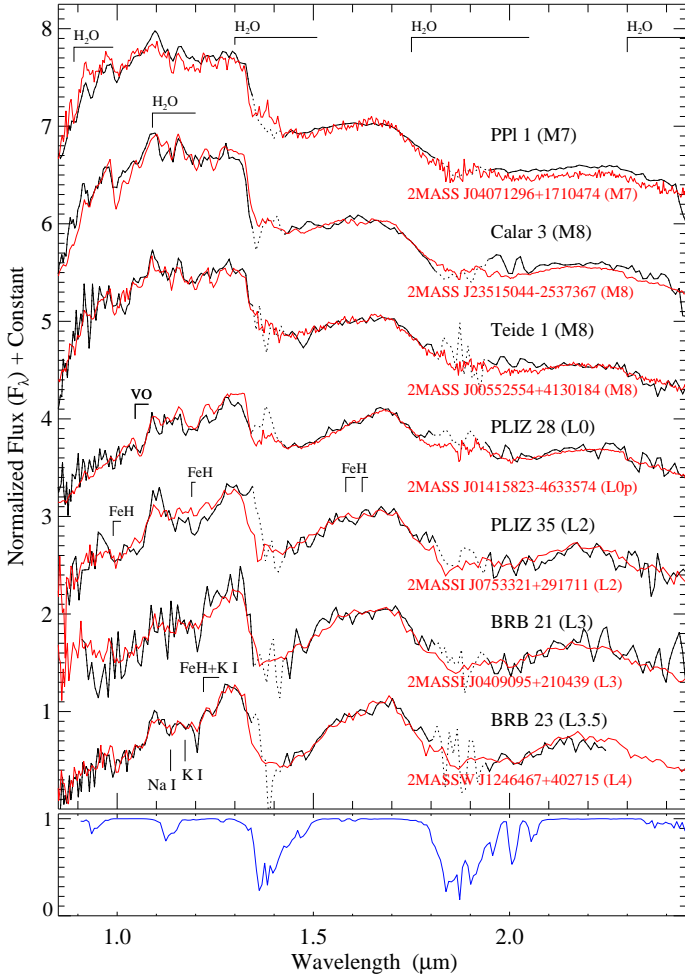


**Fig. 1.** NICS/Amici low-resolution 0.85–2.40  $\mu\text{m}$  spectra of Pleiades low-mass members (black lines). The spectra are in air wavelengths, normalized to the average flux between 1.56 and 1.74  $\mu\text{m}$ , and offset by constants. The main regions affected by tellurics are represented by dotted lines. Field dwarf spectra are overplotted in red and their references are: 2MASS J04071296+1710474 and 2MASS J00552554+4130184 (Burgasser et al. 2004), 2MASS J23515044–2537367 (Burgasser et al. 2008), 2MASS J01415823–4633574 (Kirkpatrick et al. 2006), 2MASSI J0753321+291711, 2MASSI J0409095+210439, and 2MASSW J1246467+402715 (Testi 2009). A model atmospheric transmission rebinned to a dispersion of 7  $\text{nm pix}^{-1}$  is represented in blue in the lower panel.

The Amici spectra were classified spectroscopically by comparison with spectra of the Amici (Testi et al. 2001; Testi 2009) and SpeX Prism libraries<sup>4</sup> (Adam Burgasser), with resolving power  $R \sim 100$  and *JHK*-bandpass coverage. The LIRIS spectra were classified similarly using in addition the  $R \sim 150$ –600 spec-

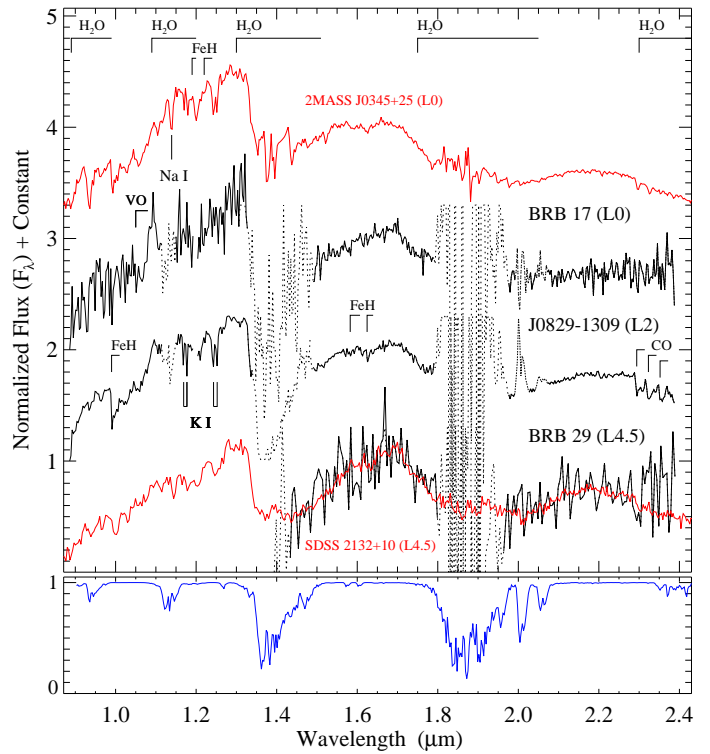


**Fig. 2.** LIRIS intermediate-resolution spectra of the Pleiades low-mass members BRB 17 and BRB 29 and the field dwarf SSSPM J0829–130 (black lines). The spectra are in air wavelengths, normalized by the average flux between 1.56 and 1.74  $\mu\text{m}$ , rebinned to dispersions of 3 (BRB 17 and SSSPM J0829–1309) and 5  $\text{nm pix}^{-1}$  (BRB 29), and offset by constants. The main regions affected by tellurics are represented by dotted lines. The spectra of the field dwarfs 2MASS J03454316+2540233 (composite spectrum of Leggett et al. 2001, rebinned to 3  $\text{nm pix}^{-1}$ ) and SDSS J213240.36+102949.4 ( $R \sim 150$ ; Chiu et al. 2006) are shown in red. A model atmospheric transmission rebinned to 3  $\text{nm pix}^{-1}$  is represented in blue in the lower panel.

tra from the L- and T-type dwarf data archive of Sandy Leggett.<sup>5</sup> The first, second, and third libraries adopt L spectral types from the far-red optical (classification scheme of Kirkpatrick et al. 1999), the far-red optical or near-infrared, and the near-infrared (classification scheme of Geballe et al. 2002, which agrees in the L0–L5 range with the optical schemes of Martín et al. 1999 and Kirkpatrick et al. 1999), respectively. For the objects of the second and third libraries, we preferentially adopted optical spectral types, when available<sup>6</sup>.

We classified the spectra first visually, considering the change in the continuum shape from the earlier to the later spectral types (e.g., the 0.85–1.3  $\mu\text{m}$  region and the  $\text{H}_2\text{O}$  absorption bands), and then by chi-squared minimization for optimization. The errors were obtained by accounting for the plausible earliest- and latest-type field dwarf spectra matching those of our targets. For BRB 17 and PLIZ 28, however, the spectra differ notably from those of normal field dwarfs. Figure 3 illustrates this with a sequence of field dwarfs, whose optical-typing references are: LP 944-20 (Kirkpatrick et al. 1999), 2MASS J12212770+0257198 (Reid et al. 2008),

<sup>5</sup> <http://staff.gemini.edu/~sleggett/LTdata.html>

<sup>6</sup> <http://www.dwarfarchives.org>

<sup>4</sup> <http://www.browndwarfs.org/spexprism>

**Table 2.** Field-dwarf- and gravity-independent spectral indices<sup>a</sup> (left and right parts of the table, respectively).

Object	sHJ (1.265–1.305, 1.60–1.70)	sKJ (1.265–1.305, 2.12–2.16)	sH <sub>2</sub> O <sup>J</sup> (1.09–1.13, 1.265–1.305)	sH <sub>2</sub> O <sup>H1</sup> (1.45–1.48, 1.60–1.70)	sH <sub>2</sub> O <sup>B</sup> (1.47–1.49, 1.59–1.61)	<SpT> <sup>b</sup>	H <sub>2</sub> O 1.5 μm (1.46–1.48, 1.57–1.59)	H <sub>2</sub> O (1.492–1.502, 1.55–1.56)	H <sub>2</sub> O-2 (2.035–2.045, 2.145–2.155)	<SpT> <sup>b</sup>
BRB 17	0.23; L2.4	0.63; L2.6	...	...	...	(L2.5)	...	1.22; L0.6	0.95; M8.4	(M9.5)
PLIZ 28	0.12; L4.5	0.51; L4.0	0.21; L3.0	0.35; L2.0	0.78; L0.8	(L3)	1.30; L1	1.17; M9.5	0.88; L0.3	(L0.5)
PLIZ 35	0.21; L2.7	0.66; L2.2	0.09; L1.2	0.37; L2.3	0.79; L0.6	(L2)	1.31; L1	1.36; L4.0	0.80; L2.6	(L2.5)
BRB 21	0.19; L3.1	0.55; L3.5	0.35; L5.2	0.38; L2.4	0.67; L3.6	(L3.5)	1.39; L2	1.42; L5.2	0.89; L0.0	(L2.5)
BRB 23	0.18; L3.4	0.55; L3.5	0.29; L4.3	0.58; L5.0	0.58; L6.2	(L4.5)	1.67; L7	1.51; L7.2	0.79; L2.8	(L5.5)
BRB 29	...	...	...	0.65; L5.8	0.68; L3.4	(L4.5)	1.56; L5	1.25; L1.3	0.68; L5.6	(L4)

(<sup>a</sup>) Spectral ranges in μm are indicated between parentheses. (<sup>b</sup>) Average spectral types derived from the spectral indices are approximated to the nearest half subclasses.

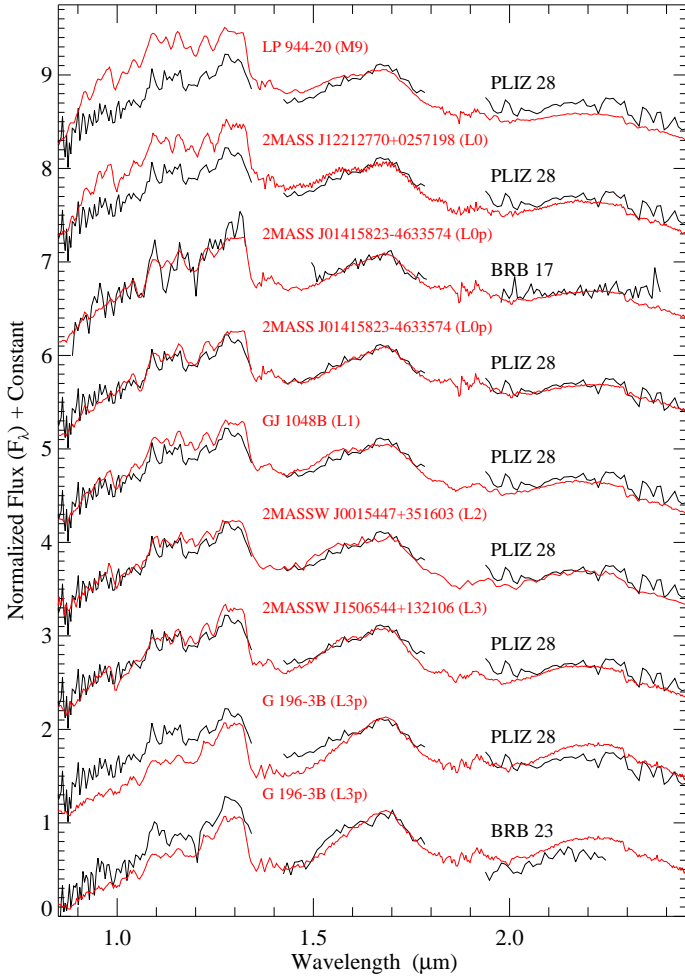


**Fig. 3.** Spectra of Pleiades L-type brown dwarfs compared to field dwarf spectra (overplotted in red). The spectra are normalized to the average flux between 1.56 and 1.74 μm and offset by constants. The LIRIS spectrum of BRB 17 is rebinned to a dispersion of 7 nm pix<sup>-1</sup>. The references of the field spectra are: LP 944-20, 2MASS J12212770+0257198, and GJ 1048B (Burgasser et al. 2008), 2MASS J01415823–4633574 (Kirkpatrick et al. 2006), 2MASSW J0015447+351603 (Testi et al. 2001), 2MASSW J1506544+132106 (Burgasser 2007), and G 196-3B (Allers et al. 2010).

2MASS J01415823–4633574 (Kirkpatrick et al. 2006, 2008; Cruz et al. 2009), GJ 1048B (Gizis et al. 2001), 2MASSW J0015447+351603 (Kirkpatrick et al. 2000),

2MASSW J1506544+132106 (Gizis et al. 2000), and G 196-3B (Cruz et al. 2009). The spectra of BRB 17 and PLIZ 28 match at best the spectrum of the low surface-gravity field dwarf 2MASS J01415823–4633574 (Kirkpatrick et al. 2006). Therefore we adopted its L0±1 (peculiar) spectral type. We compared also with G 196-3B, another low surface-gravity field dwarf (Rebolo et al. 1998; Martín et al. 1999; Kirkpatrick et al. 2001; Allers et al. 2007; Kirkpatrick et al. 2008), but the match is less good, as with any of the other Pleiades spectra. The latter compare at best with the spectra of the normal field dwarfs overplotted in Figs 1 and 2. We verified whether the  $J - H$  and  $H - K$  colours of our Pleiades targets agree with those of the specific field dwarfs providing the best spectral match. For the former objects we used UKIDSS<sup>7</sup> photometry and for the latter dwarfs we used 2MASS photometry converted to the WFCAM photometric system using the transformations of Hodgkin et al. (2009), or else when available UKIDSS- (2MASS J0409095+210439) or MKO photometry (SDSS J213240.36+102949.4; Chiu et al. 2006). On average, the colours agree within the error bars, and, in all cases but two, better than about 1.5 times the sum of the error bars. 2MASS J00552554+4130184, with  $H - K \approx 0.0$  mag, is 0.5 mag bluer than Teide 1, which is in disagreement with the very similar fluxes in the spectra of the two objects (Fig. 1). 2MASS J01415823–4633574 is 0.20 mag redder in  $H - K$  than BRB 17.

Our derived spectral types (Table 1) indicate that the low-mass brown dwarfs confirmed by proper motion in Bihain et al. (2006) are indeed ultra-cool dwarfs of spectral type L. They indicate also that our near-infrared classification of the late M-type Amici spectra is consistent with their optical spectral classification. Steele et al. (1995), Williams et al. (1996) and Greissl et al. (2007) have already presented near-infrared low-resolution spectra of Pleiades early M- to L0-type dwarfs, including PPI 1, Teide 1, Roque 33, and Roque 25, which at least qualitatively support the optical classification.

For the Pleiades L-type spectra, we measured five field-dwarf spectral indices, in regions less affected by telluric absorption bands: sHJ, sKJ, sH<sub>2</sub>O<sup>J</sup>, and sH<sub>2</sub>O<sup>H1</sup> from Testi et al. (2001) and sH<sub>2</sub>O<sup>B</sup> from Reid et al. (2001). For BRB 17, only the sHJ and sKJ indices could be measured. We note that the indices depend on narrow regions that are significantly affected by noise in our data, implying that they are less reliable than spectral comparisons using the whole regions available. The average

<sup>7</sup> UKIDSS uses the UKIRT Wide Field Camera (WFCAM; Casali et al. 2007) and a photometric system described in Hewett et al. (2006). The pipeline processing and science archive are described in Hambly et al. (2008).

spectral types derived from the field dwarf indices are shown in the left part of Table 2 and agree with our adopted spectral types (Table 1) except for BRB 17 and PLIZ 28. We also measured the H<sub>2</sub>O 1.5  $\mu$ m (Geballe et al. 2002), H<sub>2</sub>O (Allers et al. 2007), and H<sub>2</sub>O-2 (Slesnick et al. 2004) spectral indices, expected to be gravity-independent in early to mid L-types. The two latter indices are more appropriate for spectra of higher spectral resolution than the Amici data. Nevertheless, we find good agreement between the average spectral types derived from the field-dwarf and “gravity-independent” indices. In the case of PLIZ 28 and BRB 17, the spectral indices independent of the *J* band – especially the gravity-independent indices – give earlier spectral types, more consistent with the spectral type L0. This results from the apparently shallower water bands at  $\sim$ 1.4 and  $\sim$ 1.9  $\mu$ m for the relatively depressed continuum at 0.85–1.3  $\mu$ m, as compared to normal field dwarfs. Spectra of improved signal-to-noise ratio and flux correction will permit us to confirm or refute this unusual combination of spectral features.

## 4. Discussion

### 4.1. Spectroscopic properties

In Fig. 2, we compare the spectrum of the L0-type BRB 17 with those of two field dwarfs, the optical L0 standard 2MASS J03454316+2540233 of Kirkpatrick et al. (1999) and the L2-type SSSPM J0829–1309. In the blue part, the Pleiades spectrum displays the VO band at  $\sim$ 1.05  $\mu$ m, which appears more clearly than other local features (we note that the FeH band at 1.2  $\mu$ m is not covered because of bad pixel columns in the LIRIS frames). In the central part (*H* band), the shape of the continuum is triangular, instead of approximately flat-topped as in the comparison spectra. These peculiarities can also be seen in the lower resolution spectrum of PLIZ 28 (Figs. 1 and 3). Deep VO bands and triangular *H*-band continuum shapes, as well as weak FeH and CO bands and weak Na I and K I lines, have been observed in spectra of L-type objects in star-forming regions and have been associated with lower surface gravity (Martín et al. 1998b; Lucas et al. 2001; McGovern et al. 2004; Allers et al. 2007). The triangular *H*-band continuum shape could be explained by a reduction in the H<sub>2</sub> collision-induced and H<sub>2</sub>O absorptions in lower surface-gravity and dustier atmospheres (Borysow et al. 1997; Kirkpatrick et al. 2006; Mohanty et al. 2007). Possibly, the entire apparently peculiar continuum of PLIZ 28 and BRB 17 (see Sect. 3) could be explained by more dusty atmospheres (see Fig. 2 in Tsuji et al. 1996).

### 4.2. Spectrophotometric properties

We compare the spectrophotometric properties of Pleiades L-type brown dwarfs mainly with those of field dwarfs of known parallax. We use *I*<sub>C</sub>- and UKIDSS *ZYJHK*-band photometry. To our nine Pleiades targets, we add 36 other low-mass Pleiades stars and brown dwarfs with spectral type measurements (Table A.1). They are cluster members confirmed by proper motion or the lithium test (Rebolo et al. 1992), and many present spectral features of low surface gravity (see spectroscopic references in the table). We include the M9-type Roque 4 and the L0-type Roque 25, which have spectral features consistent with cluster membership (Zapatero Osorio et al. 1997; Martín et al. 1998b, 2000; Kirkpatrick et al. 2008); Roque 25 has furthermore a proper motion consistent with cluster membership (see Appendix B). To obtain *JHK*-band absolute magnitudes, we use the Pleiades revised trigonometric parallax distance of

120.2 $\pm$ 1.9 pc (van Leeuwen 2009a,b). We do not account for the distance uncertainty due to cluster depth ( $\approx$ 0.2 mag towards the cluster centre, Pinfield et al. 1998). We compute average *JHK*-band absolute magnitudes and *I*<sub>C</sub> – *J*, *Z* – *J*, and *Y* – *J* colours in the spectral type intervals [4.75+*i*/2, 5.25+*i*/2] with *i*=0...19 (where 5.0 corresponds to M5.0, 14.5 to L4.5) and excluding known binaries. We also obtain chi-squared linear fits to the *J* – *H*, *H* – *K*, and *J* – *K* colours as a function of spectral type, including these binaries.

For field dwarfs compiled with trigonometric parallaxes and – preferentially optical – spectral types (van Altena et al. 1995; Dahn et al. 2000, 2002; Henry et al. 2004; Faherty et al. 2009), we use *I*<sub>C</sub>- (Leggett et al. 2000; Dahn et al. 2000, 2002; Henry et al. 2004; Phan-Bao et al. 2008) and 2MASS or MKO *JHK*-band photometry. We convert the 2MASS photometry to the (MKO-)WFCAM system using the transformations of Hodgkin et al. (2009). For some field dwarfs, we use available WFCAM *ZYJHK*-band photometry (UKIDSS DDR6) or WFCAM *Z* – *J* and *Y* – *J* synthetic colours (Hewett et al. 2006; Rayner et al. 2009). We cautiously assume errors of 0.10 mag and 0.05 mag in the colours of the former and latter studies, respectively. Late M- and L-type close binaries resolved by imaging (see references in Faherty et al. 2009) are accounted for in the comparison. We compute average absolute magnitudes, average colours and linear fits in a similar way to the Pleiades sample, but using values with total errors smaller than 0.4 mag. For illustrative purpose, we highlight four relatively bright L4-type field dwarfs (HD 130948B and C, Potter et al. 2002; Dupuy et al. 2009; HD 49197B, Metchev & Hillenbrand 2004; 2MASSW J1841086+311727, Kirkpatrick et al. 2000) and we add five subdwarfs associated with the thick-disc or halo population (Bowler et al. 2009), three low-mass substellar members of relatively young associations (2M1207AB, Chauvin et al. 2004; Mohanty et al. 2007; Ducourant et al. 2008; AB Pic B, Chauvin et al. 2005; Bonnefoy et al. 2010), and three field dwarfs without parallaxe measurements (2MASS J01415823–4633574, G 196–3B and the candidate young L4.5-type 2MASS J18212815+1414010,Looper et al. 2008).

As claimed in Bihain et al. (2006), the Pleiades and field L-type dwarfs may have similar spectral energy distributions and luminosities, and thus possibly similar (but not necessarily equal) radii, based on the apparent overlapping of these objects in the *J* versus *I*–*J*, *J*–*H* and *J*–*K* colour–magnitude diagrams. Indeed, our near-infrared absolute magnitude versus spectral type diagrams (Fig. 4) indicate that unlike the Pleiades M-type dwarfs, the L-type dwarfs appear no brighter than a few tenths of magnitude than their field counterparts, especially in the *J* band. Nevertheless, if we adopt as in Bihain et al. (2006) the larger Pleiades distance of 133.8 $\pm$ 3.0 pc (Percival et al. 2005) – obtained by main sequence fitting in the optical and near-infrared using field dwarfs – the Pleiades L-type dwarfs would be brighter by 0.23 mag, implying less similar luminosities to those of the field dwarfs. Besides, the diagrams of Figs. 5 and 6 show no significant differences between the colours of Pleiades and field L-type dwarfs.

At the M/L transition (see Fig. 4), we note that four Pleiades brown dwarfs (NPL 40, BRB 17, PLIZ 28 and Roque 25) appear to have a relatively lower flux towards the *J* band, which could be due to a too early spectral typing or some atmospheric or interstellar extinction. The effect is stronger for the  $\sim$ 30 Myr old low-mass brown dwarf or massive planet AB Pic B, and even stronger for the later-type  $\sim$ 8 Myr few-Jupiter-mass



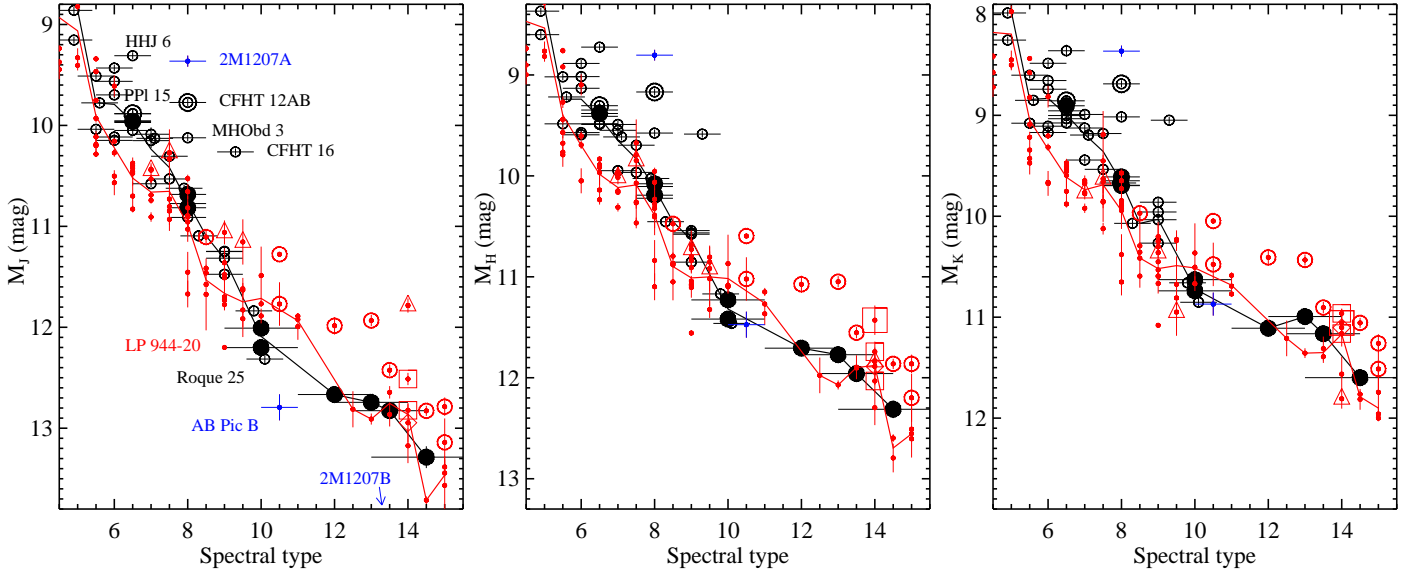


**Fig. 4.** Absolute magnitude  $M_J$ ,  $M_H$ , and  $M_K$  versus spectral type (M6=6, L0=10) diagrams (left-, middle-, and right panels, respectively), with Pleiades members (black filled circles for new data and black small open circles for previous data) and field dwarfs (red dots). Resolved close binaries are encircled. Average Pleiades and field values are represented by the black- and red solid lines, respectively. For illustrative purpose, we highlight four relatively bright field L4-type dwarfs (HD 130948B and C by small squares, HD 49197B by large square, and 2MASSW J1841086+311727 by diamond) and we add five subdwarfs (triangles) and three low-mass substellar members of very young associations (blue dots; we assume an L5 type for 2M1207B). All three diagrams span 5.0 mag. The photometry is in the MKO-WFCAM system.

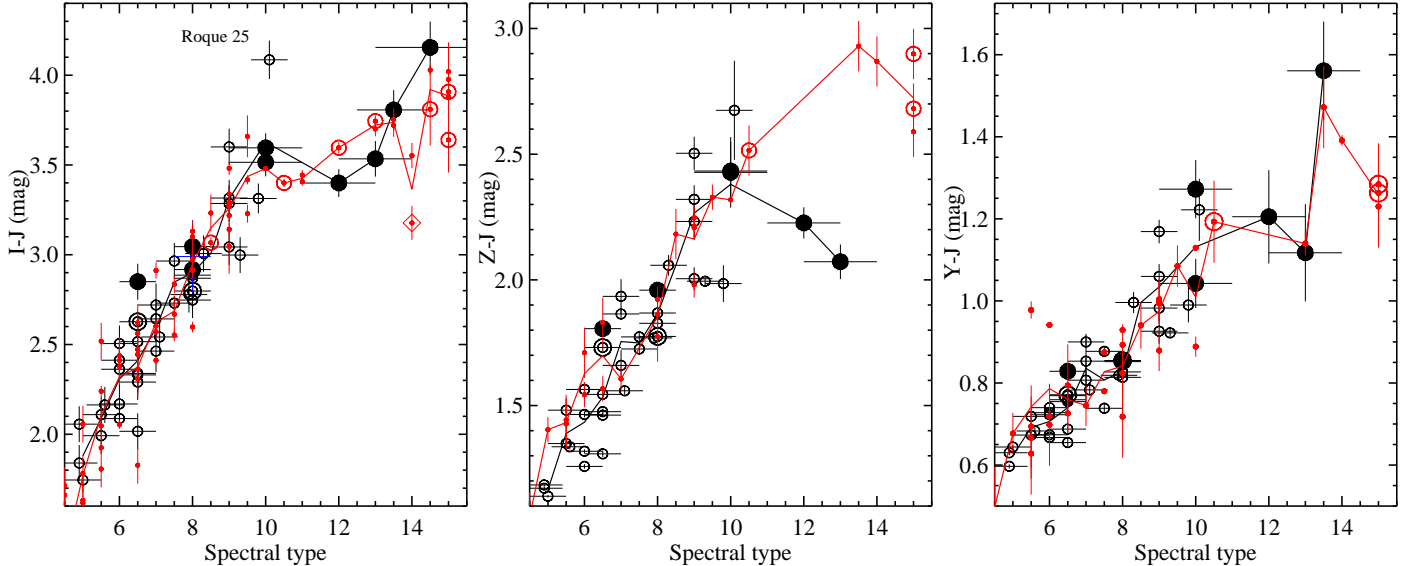


**Fig. 5.**  $I_C - J$ ,  $Z - J$ , and  $Y - J$  versus spectral type diagrams (left-, middle-, and right panels, respectively). Same symbol definitions as in Figure 4.

2M1207B<sup>8</sup>, for which ongoing accretion/formation processes have been proposed (Mohanty et al. 2007; Mamajek & Meyer 2007; Ducourant et al. 2008; Patience et al. 2010). Finally the very nearby (5 pc) M9-type field brown dwarf LP 944-20, with lithium absorption and an age estimated to be of several hundred Myr (Tinney 1998; Ribas 2003) appears also to be fainter, but equally in the  $HK$  bands as in the  $J$  band, an effect that could be real or related to uncertainties in the parallax measurement.

<sup>8</sup> 2M1207B is less luminous than the Pleiades and field dwarf sequences, by about 3, 2, and 1 magnitudes in the  $J$ ,  $H$ , and  $K$  bands, respectively, assuming a spectral type L5.

The near-infrared colour diagrams of Fig. 6 indicate that late M- and L-type Pleiades dwarfs are marginally redder in  $J - H$  and  $H - K$  than their field counterparts. The difference reaches  $0.11 \pm 0.20$  mag in  $J - K$  and at spectral type L3, using the chi-squared linear fits. If we consider only the field dwarfs with UKIDSS photometry (10 M6–L4-type dwarfs), the  $J - K$  difference at L3 increases by 0.08 mag. This suggests that the slightly redder colour is not due to some bias in the photometric transformations of Hodgkin et al. (2009). It could be associated with both:

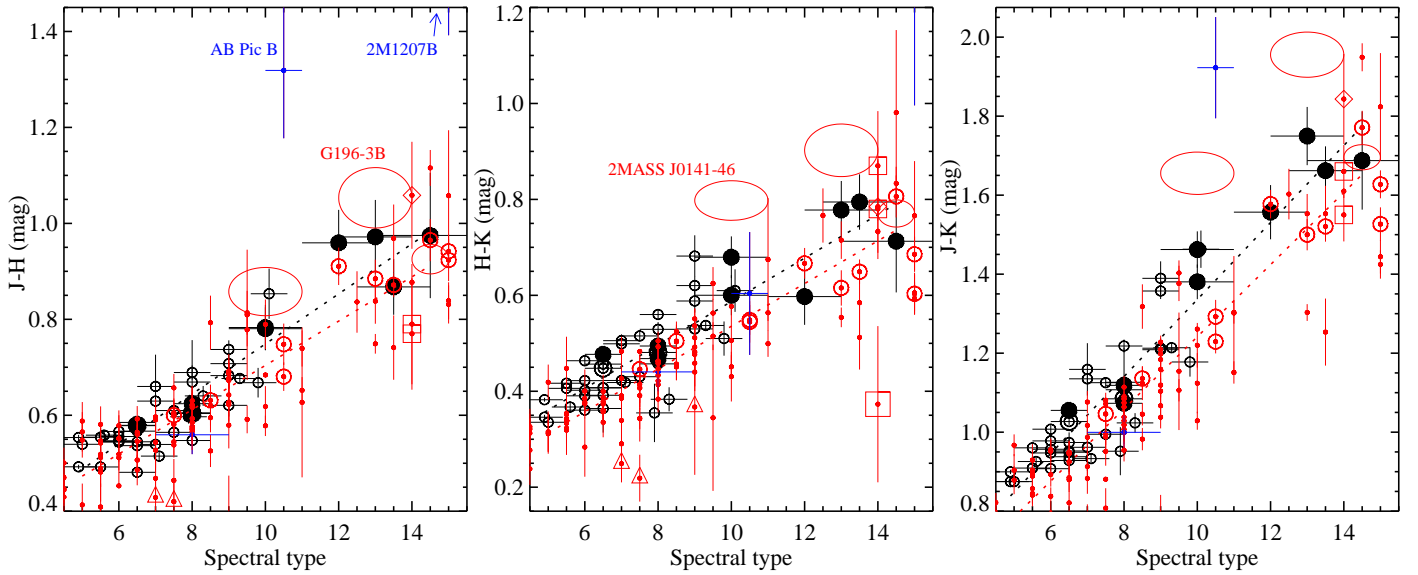


**Fig. 6.**  $J-H$ ,  $H-K$ , and  $J-K$  versus spectral type diagrams (left-, middle-, and right panels, respectively). Same symbol definitions as in Fig. 4. Pleiades and field chi-squared linear fits to the colours as a function of spectral type are represented by the *black-* and *red dashed lines*, respectively. For illustrative purpose, we add the low surface gravity field dwarfs 2MASS J01415823–4633574 and G 196–3B and the candidate young field dwarf 2MASS J18212815+1414010, represented by error *ellipses* for clarity.

1. The reddening in the line of sight of the faint Pleiades brown dwarfs. The  $E(B-V)$  values could be in the range 0.02–0.14 mag (Taylor 2008), which using the  $E(J-K_s)/E(B-V)$  relation of An et al. (2007), would lead to small infrared excesses  $E(J-K_s) = 0.01-0.09$  mag for an intrinsic colour  $(J-K_s)_0 = 1.5$  mag.
2. The youth of the Pleiades brown dwarfs. Indeed, the  $J-K$  colour is found to be larger, in average, for L-type field dwarfs with smaller velocity dispersion, and thus of younger age (Faherty et al. 2009; Schmidt et al. 2010). The 0.1 Gyr old Pleiads would likely have lower surface gravities than those of the older field dwarfs, which furthermore could have lower metallicities than the Pleiades ( $[\text{Fe}/\text{H}]_{\text{Pleiades}} = 0.03 \pm 0.05$  dex, Funayama et al. 2009; Soderblom et al. 2009). Both lower surface gravities and higher metallicities may cause lower  $\text{H}_2$  collision induced absorption or dustier atmospheres, and therefore larger  $J-K$  colours (Linsky 1969; Saumon et al. 1994; Borysow et al. 1997; Mohanty et al. 2007). Also, several field L-type dwarfs with spectral features of low surface gravity have very red near-infrared colours (see Fig. 6 and Kirkpatrick et al. 2008; Cruz et al. 2009).

#### 4.3. Hertzsprung–Russell diagram

Altogether, the L-type Pleiades and field dwarf sequences appear to be rather close in the photometric – spectral-type diagrams. We build now the Hertzsprung–Russell (HR) diagram of our sample of 45 Pleiades members. We convert observed  $J$ -band magnitudes into luminosities using the open cluster revised parallactic distance and an average of field dwarf  $J$ -band bolometric corrections  $BC_J$  (Dahn et al. 2002; Vrba et al. 2004) as a function of spectral type. The  $J$  band is chosen because the spectral energy distributions of the Pleiades objects peak in this band and the  $J-K$  colour excesses with respect to their field dwarf spectral type counterparts are only 0.1–0.2 mag. For the effective temperatures ( $T_{\text{eff}}$ ), we use an average of field dwarf  $T_{\text{eff}}$  determinations (Basri et al. 2000; Dahn et al. 2002; Vrba et al. 2004)

also as a function of spectral type. We provide the luminosity and  $T_{\text{eff}}$  values for our nine Pleiades targets in Table 3, where the error bars account for the uncertainties in the photometry, cluster distance, spectral types, and the spread in the field dwarf  $BC_J$  and  $T_{\text{eff}}$ . Figure 7 shows the Hertzsprung–Russell diagram. The Pleiades substellar sequence clearly extends to mid-L spectral types or  $T_{\text{eff}} \sim 1700$  K. The “single-object” sequence has a luminosity dispersion of about 0.1 dex (except at  $\sim \text{M9-L0}$ ) and no apparent temperature gap between 2900 and 1700 K. The sequence of suspected equal-mass binaries is clearly seen at the warmest temperatures, whereas below 2400 K there is no obvious hint of such objects, despite the fact that photometric surveys tend to be biased towards their detection.

We overplot the theoretical 120-Myr isochrones of Chabrier et al. (2000, DUSTY model) and Burrows et al. (1997) in Fig. 7. Both models make similar predictions for luminosity,  $T_{\text{eff}}$  and mass, and both appear to reproduce well the slope of the mid- to late-M single-object sequence of the Pleiades within about  $1-\sigma$  uncertainty. There is, however, a discrepancy between theory and observations in the L-type regime ( $\leq 2400$  K): our objects appear 100–400 K warmer (1–3 spectral subclasses earlier) or 0.1–0.4 dex less luminous than the isochrones. Using the  $K$  band and the field dwarf bolometric correction from Golimowski et al. (2004) increase by  $\lesssim 0.10$  dex the luminosities of the Pleiades L-type objects with the largest  $J-K$  colour excess, thus only slightly reducing the discrepancy. It is uncertain whether the field dwarf bolometric correction- and  $T_{\text{eff}}$ -spectral type relations may be valid for the Pleiades L-type brown dwarfs because of gravity dependence. However, the latter appear to have spectral energy distributions and luminosities that are in general very close to those of their field dwarf spectral type counterparts. Thus, the discrepancy in the Hertzsprung–Russell diagram may also be due to incorrect model predictions, such as an underestimation of the contraction rate of the Pleiades L-type dwarfs.

The luminosity range of the spectroscopic sample as compared to the theoretical luminosities of the 120 Myr DUSTY isochrone (Fig. 7) would imply a mass range of  $\sim 0.025-0.1 M_{\odot}$

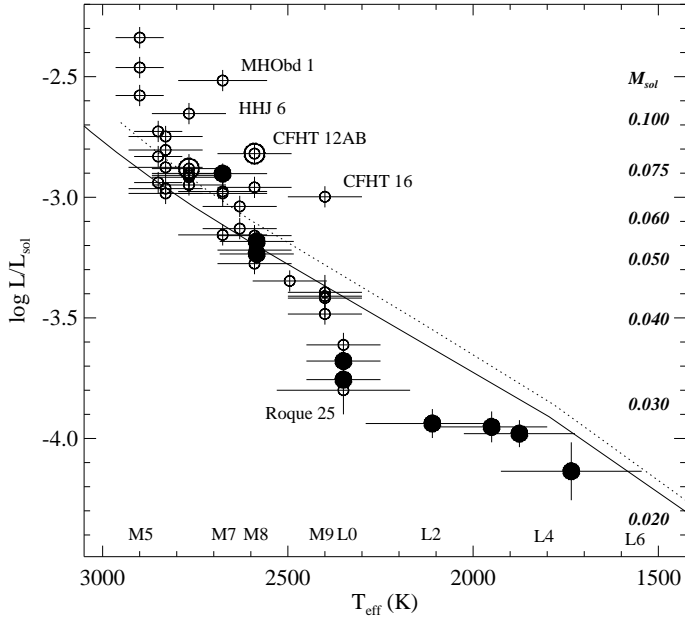


**Fig. 7.** Hertzsprung–Russell diagram of Pleiades low-mass stars and brown dwarfs. Same symbol definitions as in Figure 4. Theoretical 120 Myr isochrones of Chabrier et al. (2000, DUSTY) and Burrows et al. (1997) are represented by dotted and solid lines, respectively. Spectral types and DUSTY theoretical masses are indicated.

**Table 3.** Luminosities, effective temperatures, and masses for our Pleiades targets.

Object	SpT	$\log L/L_{\odot}$ (dex)	$T_{\text{eff}}$ (K)	$M$ ( $M_{\odot}$ )
PPI 1	M6.5±0.5	-2.90±0.04	2676±120	~0.074
Calar 3	M8.0±0.5	-3.18±0.04	2584±100	~0.054
Teide 1	M8.0±0.5	-3.24±0.04	2584±100	~0.052
BRB 17	L0.0±1.0	-3.68±0.06	2350±100	~0.035
PLIZ 28	L0.0±1.0	-3.76±0.06	2350±100	~0.033
PLIZ 35	L2.0±1.0	-3.94±0.06	2110±180	~0.028
BRB 21	L3.0±1.0	-3.95±0.06	1950±150	~0.028
BRB 23	L3.5±1.0	-3.98±0.06	1875±150	~0.027
BRB 29	L4.5±1.5	-4.14±0.12	1735±190	~0.024

(without accounting for the brightest, probable binaries). In Table 3, we list individual masses for our targets, obtained by interpolating linearly between the model points using our estimated luminosities. The faintest and coolest brown dwarf is BRB 29, with an estimated mass of  $25 \pm 8 M_{\text{Jup}}$ .

## 5. Conclusions

We obtained near-infrared NICS/Amici and LIRIS spectra of six  $J = 17.4\text{--}18.8$  mag candidate L-type brown dwarfs of the ~120 Myr old Pleiades cluster, as well as Amici spectra of three other members that are well-known late M-type brown dwarfs. We confirm that the former objects have early- to mid-L spectral types and also confirm the optical spectral types reported for the latter objects. PLIZ 28 and BRB 17, the two earliest L-type brown dwarfs, present a triangular  $H$ -band continuum shape and a noticeable VO band, associable to low surface gravity, dust and youth. The Pleiades L-type brown dwarfs appear to have similar absolute magnitudes and colours as their field counterparts,

but have slightly redder near-infrared colours, possibly related to both reddening and youth.

We build the Hertzsprung–Russell diagram of our Pleiades sample using field dwarf relations and find good agreement with theoretical models for the M5.5–9 type objects. However, for the L0–5 type brown dwarfs, models appear to overpredict the luminosity ( $\Delta \log L/L_{\odot} = 0.1 - 0.4$  dex) or underestimate the effective temperature ( $\Delta T_{\text{eff}} = 100\text{--}400$  K). It is also possible that the adopted field dwarf relations are not truly valid for ~120 Myr-old objects. Additional optical-to-infrared spectroscopy and higher resolution imaging of the Pleiades L-type brown dwarfs may allow us to account more for dust opacities and binarity (e.g., Knapp et al. 2004; Burgasser et al. 2008), and refine our estimates of spectral types, effective temperatures, luminosities, and masses. Current models predict masses in the range 0.025–0.035  $M_{\odot}$  for the Pleiades L0–5 type brown dwarfs.

*Acknowledgements.* We thank the anonymous referee for her/his valuable comments and suggestions, and Terry Mahoney for correcting the English text. We thank Katelyn N. Allers for providing the spectrum of G 196-3B. The study presented here is based on observations made with the Italian Telescopio Nazionale Galileo (TNG) and the William Herschel Telescope (WHT) operated on the island of La Palma by the Fundación Galileo Galilei of the INAF (Istituto Nazionale di Astrofisica) and the Isaac Newton Group, respectively, in the Spanish Observatorio del Roque de los Muchachos of the Instituto de Astrofísica de Canarias. We thank the TNG for allocation of director’s discretionary time to this programme. Based on observations collected at the German-Spanish Astronomical Center, Calar Alto, jointly operated by the Max-Planck-Institut für Astronomie Heidelberg and the Instituto de Astrofísica de Andalucía (CSIC). We thank Calar Alto Observatory for allocation of director’s discretionary time to this programme. This research has been supported by the Spanish Ministry of Science and Innovation (MICINN). This research has benefited from the SpeX Prism Spectral Libraries maintained by Adam Burgasser, the L and T dwarf data archive maintained by Sandy K. Leggett, and the M, L, and T dwarf compendium housed at DwarfArchives.org and maintained by Chris Gelino, Davy Kirkpatrick, and Adam Burgasser. This research has made use of SAOImage DS9, developed by Smithsonian Astrophysical Observatory. This research has made use of the SIMBAD database, operated at CDS, Strasbourg, France. This publication makes use of data products from the Two Micron All Sky Survey, which is a joint project of the University of Massachusetts and the Infrared Processing and Analysis centre/California Institute of Technology, funded by the National Aeronautics and Space Administration and the National Science Foundation. This research has made use of NASA’s Astrophysics Data System Bibliographic Services.

## References

- Abazajian, K. N., Adelman-McCarthy, J. K., Agüeros, M. A., et al. 2009, *ApJS*, 182, 543
- Allen, P. R., Koerner, D. W., Reid, I. N., & Trilling, D. E. 2005, *ApJ*, 625, 385
- Allers, K. N., Jaffe, D. T., Luhman, K. L., et al. 2007, *ApJ*, 657, 511
- Allers, K. N., Liu, M. C., Dupuy, T. J., & Cushing, M. C. 2010, *ApJ*, 715, 561
- An, D., Terndrup, D. M., & Pinsonneault, M. H. 2007, *ApJ*, 671, 1640
- Bannister, N. P. & Jameson, R. F. 2007, *MNRAS*, 378, L24
- Barrado y Navascués, D., Zapatero Osorio, M. R., Béjar, V. J. S., et al. 2001, *A&A*, 377, L9
- Barrado y Navascués, D., Zapatero Osorio, M. R., Martín, E. L., et al. 2002, *A&A*, 393, L85
- Basri, G., Marcy, G. W., & Graham, J. R. 1996, *ApJ*, 458, 600
- Basri, G., Mohanty, S., Allard, F., et al. 2000, *ApJ*, 538, 363
- Béjar, V. J. S., Martín, E. L., Zapatero Osorio, M. R., et al. 2001, *ApJ*, 556, 830
- Béjar, V. J. S., Zapatero Osorio, M. R., Pérez-Garrido, A., et al. 2008, *ApJ*, 673, L185
- Bihain, G., Rebolo, R., Béjar, V. J. S., et al. 2006, *A&A*, 458, 805
- Bonnefoy, M., Chauvin, G., Rojo, P., et al. 2010, *A&A*, 512, A52
- Borysow, A., Jorgensen, U. G., & Zheng, C. 1997, *A&A*, 324, 185
- Bouvier, J., Stauffer, J. R., Martín, E. L., et al. 1998, *A&A*, 336, 490
- Bowler, B. P., Liu, M. C., & Cushing, M. C. 2009, *ApJ*, 706, 1114
- Burgasser, A. J. 2004, *ApJS*, 155, 191
- Burgasser, A. J. 2007, *ApJ*, 659, 655
- Burgasser, A. J., Liu, M. C., Ireland, M. J., Cruz, K. L., & Dupuy, T. J. 2008, *ApJ*, 681, 579
- Burgasser, A. J., McElwain, M. W., Kirkpatrick, J. D., et al. 2004, *AJ*, 127, 2856
- Burrows, A., Marley, M., Hubbard, W. B., et al. 1997, *ApJ*, 491, 856



- Casali, M., Adamson, A., Alves de Oliveira, C., et al. 2007, *A&A*, 467, 777
- Casewell, S. L., Dobbie, P. D., Hodgkin, S. T., et al. 2007, *MNRAS*, 378, 1131
- Casewell, S. L., Jameson, R. F., & Burleigh, M. R. 2008, *MNRAS*, 390, 1517
- Chabrier, G. 2002, *ApJ*, 567, 304
- Chabrier, G. 2003, *PASP*, 115, 763
- Chabrier, G., Baraffe, I., Allard, F., & Hauschildt, P. 2000, *ApJ*, 542, 464
- Chauvin, G., Lagrange, A.-M., Dumas, C., et al. 2004, *A&A*, 425, L29
- Chauvin, G., Lagrange, A.-M., Zuckerman, B., et al. 2005, *A&A*, 438, L29
- Chiu, K., Fan, X., Leggett, S. K., et al. 2006, *AJ*, 131, 2722
- Cosburn, M. R., Hodgkin, S. T., Jameson, R. F., & Pinfield, D. J. 1997, *MNRAS*, 288, L23
- Cruz, K. L., Kirkpatrick, J. D., & Burgasser, A. J. 2009, *AJ*, 137, 3345
- Cushing, M. C., Rayner, J. T., & Vacca, W. D. 2005, *ApJ*, 623, 1115
- Dahn, C. C., Guetter, H. H., Harris, H. C., et al. 2000, in *ASP Conf. Ser.* 212: From Giant Planets to Cool Stars, 74
- Dahn, C. C., Harris, H. C., Vrba, F. J., et al. 2002, *AJ*, 124, 1170
- Deacon, N. R. & Hambly, N. C. 2004, *A&A*, 416, 125
- Ducourant, C., Teixeira, R., Chauvin, G., et al. 2008, *A&A*, 477, L1
- Dupuy, T. J., Liu, M. C., & Ireland, M. J. 2009, *ApJ*, 692, 729
- Faherty, J. K., Burgasser, A. J., Cruz, K. L., et al. 2009, *AJ*, 137, 1
- Festini, L. 1998a, *A&A*, 333, 497
- Festini, L. 1998b, *MNRAS*, 298, L34
- Funayama, H., Itoh, Y., Oasa, Y., et al. 2009, *PASJ*, 61, 930
- Geballe, T. R., Knapp, G. R., Leggett, S. K., et al. 2002, *ApJ*, 564, 466
- Gizis, J. E. 2002, *ApJ*, 575, 484
- Gizis, J. E., Kirkpatrick, J. D., & Wilson, J. C. 2001, *AJ*, 121, 2185
- Gizis, J. E., Monet, D. G., Reid, I. N., et al. 2000, *AJ*, 120, 1085
- Golimowski, D. A., Leggett, S. K., Marley, M. S., et al. 2004, *AJ*, 127, 3516
- Greissl, J., Meyer, M. R., Wilking, B. A., et al. 2007, *AJ*, 133, 1321
- Hambly, N. C., Collins, R. S., Cross, N. J. G., et al. 2008, *MNRAS*, 384, 637
- Hambly, N. C., Hawkins, M. R. S., & Jameson, R. F. 1993, *A&AS*, 100, 607
- Hammersley, P. L. 1998, *New Astronomy Review*, 42, 533
- Henry, T. J., Subasavage, J. P., Brown, M. A., et al. 2004, *AJ*, 128, 2460
- Hewett, P. C., Warren, S. J., Leggett, S. K., & Hodgkin, S. T. 2006, *MNRAS*, 367, 454
- Hodgkin, S. T., Irwin, M. J., Hewett, P. C., & Warren, S. J. 2009, *MNRAS*, 394, 675
- Itoh, Y., Hayashi, M., Tamura, M., et al. 2005, *ApJ*, 620, 984
- Jameson, R. F., Casewell, S. L., Bannister, N. P., et al. 2008, *MNRAS*, 384, 1399
- Jameson, R. F., Dobbie, P. D., Hodgkin, S. T., & Pinfield, D. J. 2002, *MNRAS*, 335, 853
- Jayawardhana, R. & Ivanov, V. D. 2006a, *Science*, 313, 1279
- Jayawardhana, R. & Ivanov, V. D. 2006b, *ApJ*, 647, L167
- Kirkpatrick, J. D., Barman, T. S., Burgasser, A. J., et al. 2006, *ApJ*, 639, 1120
- Kirkpatrick, J. D., Cruz, K. L., Barman, T. S., et al. 2008, *ApJ*, 689, 1295
- Kirkpatrick, J. D., Dahn, C. C., Monet, D. G., et al. 2001, *AJ*, 121, 3235
- Kirkpatrick, J. D., Reid, I. N., Liebert, J., et al. 1999, *ApJ*, 519, 802
- Kirkpatrick, J. D., Reid, I. N., Liebert, J., et al. 2000, *AJ*, 120, 447
- Knapp, G. R., Leggett, S. K., Fan, X., et al. 2004, *AJ*, 127, 3553
- Kroupa, P. & Bouvier, J. 2003, *MNRAS*, 346, 369
- Lafrenière, D., Jayawardhana, R., & van Kerkwijk, M. H. 2008, *ApJ*, 689, L153
- Lawrence, A., Warren, S. J., Almaini, O., et al. 2007, *MNRAS*, 379, 1599
- Leggett, S. K., Allard, F., Dahn, C., et al. 2000, *ApJ*, 535, 965
- Leggett, S. K., Allard, F., Geballe, T. R., Hauschildt, P. H., & Schweitzer, A. 2001, *ApJ*, 548, 908
- Linsky, J. L. 1969, *ApJ*, 156, 989
- Lodieu, N., Caux, E., Monin, J.-L., & Klotz, A. 2002, *A&A*, 383, L15
- Lodieu, N., Dobbie, P. D., Deacon, N. R., et al. 2007, *MNRAS*, 380, 712
- Lodieu, N., Hambly, N. C., Jameson, R. F., & Hodgkin, S. T. 2008, *MNRAS*, 383, 1385
- Lodieu, N., Scholz, R., McCaughrean, M. J., et al. 2005, *A&A*, 440, 1061
- Looper, D. L., Burgasser, A. J., Kirkpatrick, J. D., & Swift, B. J. 2007, *ApJ*, 669, L97
- Looper, D. L., Kirkpatrick, J. D., Cutri, R. M., et al. 2008, *ApJ*, 686, 528
- Lucas, P. W., Roche, P. F., Allard, F., & Hauschildt, P. H. 2001, *MNRAS*, 326, 695
- Lucas, P. W., Weights, D. J., Roche, P. F., & Riddick, F. C. 2006, *MNRAS*, 373, L60
- Luhman, K. L., Allen, L. E., Allen, P. R., et al. 2008, *ApJ*, 675, 1375
- Luhman, K. L., Mamajek, E. E., Allen, P. R., & Cruz, K. L. 2009, *ApJ*, 703, 399
- Luhman, K. L. & Muench, A. A. 2008, *ApJ*, 684, 654
- Luhman, K. L., Wilson, J. C., Brandner, W., et al. 2006, *ApJ*, 649, 894
- Mamajek, E. E. & Meyer, M. R. 2007, *ApJ*, 668, L175
- Martín, E. L., Basri, G., Gallegos, J. E., et al. 1998a, *ApJ*, 499, L61
- Martín, E. L., Basri, G., Zapatero Osorio, M. R., Rebolo, R., & López, R. J. G. 1998b, *ApJ*, 507, L41
- Martín, E. L., Brandner, W., Bouvier, J., et al. 2000, *ApJ*, 543, 299
- Martín, E. L., Delfosse, X., Basri, G., et al. 1999, *AJ*, 118, 2466
- Martín, E. L., Rebolo, R., & Zapatero Osorio, M. R. 1996, *ApJ*, 469, 706
- Martín, E. L., Zapatero Osorio, M. R., Barrado y Navascués, D., Béjar, V. J. S., & Rebolo, R. 2001, *ApJ*, 558, L117
- McElwain, M. W., Metchev, S. A., Larkin, J. E., et al. 2007, *ApJ*, 656, 505
- McGovern, M. R., Kirkpatrick, J. D., McLean, I. S., et al. 2004, *ApJ*, 600, 1020
- Metchev, S. A. & Hillenbrand, L. A. 2004, *ApJ*, 617, 1330
- Mohanty, S., Jayawardhana, R., Huélamo, N., & Mamajek, E. 2007, *ApJ*, 657, 1064
- Moraux, E., Bouvier, J., & Stauffer, J. R. 2001, *A&A*, 367, 211
- Moraux, E., Bouvier, J., Stauffer, J. R., & Cuillandre, J.-C. 2003, *A&A*, 400, 891
- Neuhäuser, R., Guenther, E. W., Wuchterl, G., et al. 2005, *A&A*, 435, L13
- Patience, J., King, R. R., De Rosa, R. J., & Marois, C. 2010, *A&A* in press, DOI: 10.1051/0004-6361/201014173
- Percival, S. M., Salaris, M., & Groenewegen, M. A. T. 2005, *A&A*, 429, 887
- Phan-Bao, N., Bessell, M. S., Martín, E. L., et al. 2008, *MNRAS*, 383, 831
- Pinfield, D. J., Dobbie, P. D., Jameson, R. F., et al. 2003, *MNRAS*, 342, 1241
- Pinfield, D. J., Hodgkin, S. T., Jameson, R. F., et al. 2000, *MNRAS*, 313, 347
- Pinfield, D. J., Jameson, R. F., & Hodgkin, S. T. 1998, *MNRAS*, 299, 955
- Pinfield, D. J., Jones, H. R. A., Lucas, P. W., et al. 2006, *MNRAS*, 368, 1281
- Potter, D., Martín, E. L., Cushing, M. C., et al. 2002, *ApJ*, 567, L133
- Rayner, J. T., Cushing, M. C., & Vacca, W. D. 2009, *ApJS*, 185, 289
- Rebolo, R., Martín, E. L., Basri, G., Marcy, G. W., & Zapatero Osorio, M. R. 1996, *ApJ*, 469, L53
- Rebolo, R., Martín, E. L., & Magazzù, A. 1992, *ApJ*, 389, L83
- Rebolo, R., Zapatero Osorio, M. R., Madruga, S., et al. 1998, *Science*, 282, 1309
- Reid, I. N., Burgasser, A. J., Cruz, K. L., Kirkpatrick, J. D., & Gizis, J. E. 2001, *AJ*, 121, 1710
- Reid, I. N., Cruz, K. L., Kirkpatrick, J. D., et al. 2008, *AJ*, 136, 1290
- Reid, I. N., Kirkpatrick, J. D., Liebert, J., et al. 1999, *ApJ*, 521, 613
- Ribas, I. 2003, *A&A*, 400, 297
- Robichon, N., Arenou, F., Mermilliod, J.-C., & Turon, C. 1999, *A&A*, 345, 471
- Saumon, D., Bergeron, P., Lunine, J. I., Hubbard, W. B., & Burrows, A. 1994, *ApJ*, 424, 333
- Schmidt, S. J., West, A. A., Hawley, S. L., & Pineda, J. S. 2010, *AJ*, 139, 1808
- Schmidt, T. O. B., Neuhäuser, R., Seifahrt, A., et al. 2008, *A&A*, 491, 311
- Scholz, R.-D. & Meusinger, H. 2002, *MNRAS*, 336, L49
- Skrutskie, M. F., Cutri, R. M., Stiening, R., et al. 2006, *AJ*, 131, 1163
- Slesnick, C. L., Hillenbrand, L. A., & Carpenter, J. M. 2004, *ApJ*, 610, 1045
- Soderblom, D. R., Laskar, T., Valenti, J. A., Stauffer, J. R., & Rebull, L. M. 2009, *AJ*, 138, 1292
- Stauffer, J. R., Hamilton, D., & Probst, R. G. 1994, *AJ*, 108, 155
- Stauffer, J. R., Hartmann, L. W., Fazio, G. G., et al. 2007, *ApJS*, 172, 663
- Stauffer, J. R., Schild, R., Barrado y Navascués, D., et al. 1998a, *ApJ*, 504, 805
- Stauffer, J. R., Schultz, G., & Kirkpatrick, J. D. 1998b, *ApJ*, 499, L199
- Steele, I. A. & Jameson, R. F. 1995, *MNRAS*, 272, 630
- Steele, I. A., Jameson, R. F., Hodgkin, S. T., & Hambly, N. C. 1995, *MNRAS*, 275, 841
- Taylor, B. J. 2008, *AJ*, 136, 1388
- Testi, L. 2009, *A&A*, 503, 639
- Testi, L., D'Antona, F., Ghinassi, F., et al. 2001, *ApJ*, 552, L147
- Tinney, C. G. 1998, *MNRAS*, 296, L42
- Tsuji, T., Ohnaka, K., & Aoki, W. 1996, *A&A*, 305, L1
- van Altena, W. F., Lee, J. T., & Hoffleit, E. D. 1995, *The general catalogue of trigonometric [stellar] parallaxes*, ed. L. J. T., H. E. D. van Altena, W. F. van Leeuwen, F. 2009a, *A&A*, 497, 209
- van Leeuwen, F. 2009b, *A&A*, 500, 505
- Vrba, F. J., Henden, A. A., Luginbuhl, C. B., et al. 2004, *AJ*, 127, 2948
- Weights, D. J., Lucas, P. W., Roche, P. F., Pinfield, D. J., & Riddick, F. 2009, *MNRAS*, 392, 817
- Williams, D. M., Boyle, R. P., Morgan, W. T., et al. 1996, *ApJ*, 464, 238
- Zapatero Osorio, M. R., Béjar, V. J. S., Martín, E. L., et al. 2000, *Science*, 290, 103
- Zapatero Osorio, M. R., Béjar, V. J. S., Rebolo, R., Martín, E. L., & Basri, G. 1999a, *ApJ*, 524, L115
- Zapatero Osorio, M. R., Rebolo, R., Martín, E. L., et al. 1997, *ApJ*, 491, L81
- Zapatero Osorio, M. R., Rebolo, R., Martín, E. L., et al. 1999b, *A&AS*, 134, 537

## Appendix A: Pleiades spectroscopic sample of low-mass stars and brown dwarfs

## Appendix B: Cluster membership confirmation of Roque 25 by proper motion

As part of the project to characterize the Pleiades L-type population by both proper motion and spectroscopy, we obtained

*H*-band imaging data of Roque 25, the first L-type object identified in the Pleiades (Martín et al. 1998b, 2000), to assess its cluster membership by proper motion. The observations were done on the night of 2006 February 15 with the Omega-2000 instrument ( $15.4 \times 15.4$  arcmin<sup>2</sup>,  $0.45$  arcsec pix<sup>-1</sup>) mounted at the 3.5 m Telescope (Centro Astronómico Hispano-Alemán de Calar Alto, Spain). They consisted of  $1.6$  s  $\times$  23 coadds  $\times$  36 dithers on the science target, as well as dome flats. These data were reduced as in Bihain et al. (2006). We performed aperture and point-spread-function (PSF) photometry using routines within the DAOPHOT package. The *H*-band photometry was calibrated using 341 stellar sources from UKIDSS GCS DDR6, with aperture corrected magnitudes of errors  $\sigma_H(\text{UKIDSS}) < 0.1$  mag (2.0 arcsec aperture diameter). The photometry has an average relative calibration error of 0.04 mag. For Roque 25, we measure  $H = 16.85 \pm 0.05$  mag, in agreement with  $H(\text{UKIDSS}) = 16.86 \pm 0.04$  mag. Using the Omega-2000 image of Roque 25 and the discovery *I*-band image (Zapatero Osorio et al. 1999b), corresponding to a time baseline of 10.01 yr, and the method described in Bihain et al. (2006), we obtain a proper motion  $(\mu_\alpha \cos \delta, \mu_\delta) = (27.4 \pm 7.3, -32.6 \pm 3.9)$  mas yr<sup>-1</sup>. Considering the average cluster proper motion  $(\mu_\alpha \cos \delta, \mu_\delta) = (19.15 \pm 0.23, -45.72 \pm 0.18)$  mas yr<sup>-1</sup> (Robichon et al. 1999) and the fact that the low mass cluster members have a larger intrinsic velocity dispersion than that of the high mass members (Pinfield et al. 1998; Bihain et al. 2006), our result confirms that Roque 25 is also a Pleiades member by proper motion.

**Table A.1.** Pleiades spectroscopic sample of 45 low-mass stars and brown dwarfs.

Object	SpT	$\alpha^a$	$\delta^a$	$I_C$ (mag)	$Z^b$ (mag)	$Y^b$ (mag)	$J^b$ (mag)	$H^b$ (mag)	$K^b$ (mag)	Ref. <sup>c</sup>
HHJ 2	M6.5	03 38 27.52	25 30 18.1	17.30	16.591±0.011	15.938±0.007	15.284±0.007	14.747±0.005	14.355±0.006	1,-,1,7
HHJ 3	M6.0	03 48 50.45	22 44 29.9	17.51	16.562±0.010	15.825±0.006	15.098±0.006	14.531±0.005	14.141±0.004	1,-,1,7
HHJ 6	M6.5	03 41 42.41	23 54 57.1	17.00	16.171±0.007	15.464±0.006	14.709±0.004	14.124±0.004	13.760±0.050	1,-,1,7
HHJ 7	M6.0	03 57 49.37	22 08 31.0	17.00	16.149±0.007	15.498±0.005	14.831±0.005	14.286±0.005	13.884±0.003	1,-,1,7
PPI 1	M6.5	03 45 41.27	23 54 09.8	18.21	17.166±0.014	16.189±0.008	15.360±0.006	14.782±0.005	14.305±0.006	4,8,7,5
PPI 14	M5.5	03 44 34.30	23 51 24.6	17.43	16.920±0.011	16.157±0.007	15.438±0.007	14.884±0.005	14.478±0.006	4,2,7,1
PPI 15	M6.5	03 48 04.66	23 39 30.2	17.91	17.014±0.012	16.054±0.007	15.283±0.006	14.704±0.005	14.256±0.006	4,2,7,2
Calar 3	M8.0	03 51 25.57	23 45 21.3	19.00	...	...	16.083±0.010	15.478±0.009	15.009±0.011	4,3,5,3
Teide 1	M8.0	03 47 17.92	24 22 31.7	19.26	18.174±0.029	17.067±0.013	16.215±0.010	15.591±0.009	15.096±0.011	4,3,5,2
PIZ 1	M9.0	03 48 31.52	24 34 37.3	20.00	19.218±0.065	17.883±0.025	16.715±0.015	15.977±0.012	15.357±0.014	5,-,7,6
Roque 4 <sup>d</sup>	M9.0	03 43 53.55	24 31 11.6	20.25	18.970±0.054	17.709±0.025	16.649±0.016	15.942±0.016	15.260±0.040	6,-,-,5
Roque 11	M8.0	03 47 12.08	24 28 31.7	19.06	...	16.988±0.013	16.174±0.087	15.505±0.009	15.048±0.012	6,-,8,2
Roque 13	M7.5	03 45 50.66	24 09 03.5	18.67	17.478±0.017	16.582±0.010	15.705±0.008	15.095±0.006	14.580±0.008	6,8,7,5
Roque 14	M7.0	03 46 42.98	24 24 50.7	18.27	17.484±0.018	16.403±0.009	15.550±0.066	14.890±0.006	14.391±0.007	6,-,8,7
Roque 16	M6.0	03 47 39.02	24 36 22.2	17.91	17.112±0.013	16.271±0.008	15.548±0.007	14.992±0.006	14.570±0.008	6,8,7,3
Roque 17	M6.5	03 47 23.97	22 42 37.4	17.87	...	16.123±0.008	15.354±0.007	14.809±0.006	14.402±0.007	6,-,2,7
Teide 2	M6.0	03 52 06.72	24 16 00.5	18.02	17.079±0.013	16.255±0.009	15.515±0.008	14.971±0.008	14.507±0.008	7,7,7,3
CFHT 9	M6.5	03 49 15.12	24 36 22.5	17.71	16.847±0.011	16.059±0.007	15.371±0.006	14.890±0.005	14.433±0.007	8,8,7,3
CFHT 10	M6.5	03 44 32.32	25 25 18.0	17.78	16.994±0.012	16.209±0.009	15.450±0.008	14.883±0.007	14.476±0.007	8,8,7,3
CFHT 12	M8.0	03 53 55.12	23 23 36.2	17.97	16.947±0.012	16.027±0.007	15.172±0.006	14.569±0.005	14.088±0.005	8,8,3,3
CFHT 15	M7.0	03 55 12.60	23 17 37.3	18.62	17.842±0.022	16.877±0.012	15.977±0.010	15.348±0.009	14.842±0.010	8,8,3,3
MHObd 3	M8.0	03 41 54.16	23 05 04.7	18.27	17.349±0.016	16.376±0.010	15.522±0.008	14.975±0.007	14.415±0.007	8,8,7,4
NPL 26	M5.0	03 47 07.89	24 23 37.9	15.70	15.094±0.004	14.598±0.003	13.954±0.003	13.415±0.002	13.080±0.002	9,-,4,2
NPL 34	M6.0	03 48 55.65	24 21 40.1	17.05	16.220±0.007	15.636±0.005	14.963±0.005	14.416±0.004	14.055±0.005	9,-,1,2
NPL 36	M7.5	03 48 19.02	24 25 12.7	18.66	17.655±0.020	16.668±0.011	15.930±0.009	15.365±0.008	14.935±0.011	9,-,7,2
NPL 38	M8.0	03 47 50.41	23 54 47.9	19.18	18.179±0.028	17.138±0.014	16.311±0.011	15.622±0.009	15.093±0.012	9,-,8,2
MHObd 1	M7.0	03 44 52.42	24 36 49.5	17.95	17.147±0.014	16.294±0.008	15.487±0.059	14.948±0.006	14.525±0.007	10,10,-,4
Roque 5	M9.0	03 44 22.44	23 39 01.3	20.19	19.107±0.064	17.857±0.025	16.874±0.017	16.254±0.016	15.666±0.018	11,-,7,5
CFHT 1	M4.9	03 51 51.56	23 34 49.1	16.10	15.431±0.005	14.857±0.004	14.260±0.003	13.768±0.003	13.385±0.003	12,-,3,3
CFHT 2	M4.9	03 52 44.29	23 54 15.0	16.61	15.738±0.005	15.184±0.004	14.554±0.004	14.000±0.004	13.654±0.004	12,-,3,3
CFHT 5	M5.5	03 48 44.69	24 37 23.5	17.02	16.260±0.008	15.584±0.005	14.911±0.005	14.419±0.004	14.002±0.005	12,-,7,3
CFHT 7	M5.6	03 52 05.83	24 17 31.0	17.34	16.512±0.009	15.860±0.007	15.176±0.006	14.618±0.006	14.251±0.007	12,-,7,3
CFHT 16	M9.3	03 44 35.16	25 13 42.8	18.66	17.656±0.020	16.584±0.010	15.662±0.007	14.985±0.006	14.448±0.008	12,12,7,3
CFHT 17	M7.9	03 43 00.17	24 43 52.3	18.80	17.791±0.021	16.841±0.013	16.022±0.010	15.425±0.010	15.070±0.060	12,-,3,3
CFHT 25	M9.0	03 54 05.35	23 33 59.3	19.69	18.651±0.041	17.573±0.024	16.647±0.018	15.964±0.016	15.434±0.017	12,-,3,3
NPL 40	M9.8	03 48 49.03	24 20 25.4	20.55	19.222±0.069	18.227±0.035	17.237±0.023	16.569±0.020	16.059±0.029	12,-,8,2
Roque 7	M8.3	03 43 40.31	24 30 11.2	19.50	18.552±0.038	17.490±0.021	16.494±0.014	15.853±0.015	15.470±0.020	12,-,3,3
Roque 25	L0.1	03 48 30.75	22 44 50.4	21.80	20.389±0.193	18.936±0.065	17.714±0.039	16.861±0.035	16.251±0.027	12,-,9,5
BPL 327	M7.1	03 55 23.08	24 49 04.9	18.07	17.087±0.014	16.311±0.009	15.528±0.008	15.013±0.007	14.595±0.008	13,-,6,5
BRB 17	L0.0	03 54 07.98	23 54 27.9	20.92	19.841±0.111	18.451±0.050	17.408±0.033	16.628±0.030	16.028±0.029	14,-,5,6
PLIZ 28	L0.0	03 54 14.06	23 17 52.0	21.20	20.028±0.136	18.873±0.062	17.601±0.035	16.818±0.031	16.138±0.030	14,-,5,6
PLIZ 35	L2.0	03 52 39.16	24 46 29.5	21.46	20.292±0.030	19.271±0.100	18.066±0.055	17.106±0.042	16.509±0.042	14,-,5,6
BRB 21	L3.0	03 54 10.27	23 41 40.2	21.68	20.215±0.030	19.260±0.101	18.143±0.062	17.171±0.046	16.393±0.040	14,-,5,6
BRB 23	L3.5	03 50 39.54	25 02 54.7	22.03	...	19.786±0.112	18.225±0.044	17.358±0.038	16.563±0.043	14,-,5,6
BRB 29	L4.5	03 54 01.43	23 49 57.7	22.84	...	...	18.686±0.103	17.711±0.081	16.999±0.070	14,-,5,6

<sup>(a)</sup> Coordinates from UKIDSS Galaxy Cluster Survey DDR6.

<sup>(b)</sup> *ZYJHK*-band photometry from UKIDSS Galaxy Cluster Survey DDR6, except for the measurements at *Z* band of PLIZ 35 and BRB 21 (Casewell et al. 2007), MKO *K* band of HHJ 6, Roque 4, CFHT 17, and Roque 7 (Pinfield et al. 2003), and *J* band of MHObd 1 (2MASS, converted to UKIDSS photometric system).

<sup>(c)</sup> References for the quadruplet (SpT, Li,  $\mu$ ,  $I_C$ ):

*Spectral type or lithium test*: 1) Steele & Jameson (1995), 2) Basri et al. (1996), 3) Rebolo et al. (1996), 4) Martín et al. (1996), 5) Cossburn et al. (1997), 6) Zapatero Osorio et al. (1997), 7) Martín et al. (1998a), 8) Stauffer et al. (1998b), 9) Festin (1998b), 10) Stauffer et al. (1998a), 11) Martín et al. (1998b), 12) Martín et al. (2000), 13) Pinfield et al. (2003), 14) this study. Spectral type uncertainties for our L-type targets are listed in Table 1; for the other objects the uncertainties are typically of half a subclass.

*Proper motion*: 1) Hambly et al. (1993), 2) Pinfield et al. (2000), 3) Moraux et al. (2001), 4) Deacon & Hambly (2004), 5) Bihain et al. (2006), 6) Casewell et al. (2007), 7) Lodieu et al. (2007), 8) Stauffer et al. (2007), 9) this study.

*$I_C$ -band photometry*: 1) Stauffer et al. (1994), 2) Festin (1998a), 3) Bouvier et al. (1998), 4) Stauffer et al. (1998a), 5) Jameson et al. (2002), 6) Bihain et al. (2006), 7) Stauffer et al. (2007). Magnitude errors are of 0.05-0.1 mag.

<sup>(d)</sup> Roque 4 has radial velocity and spectral features consistent with cluster membership (Zapatero Osorio et al. 1997; Kirkpatrick et al. 2008).